



# Electrolytic coloration and spectral properties of OH<sup>-</sup>-doped KBr polycrystals

Hongen Gu<sup>a,\*</sup>, Jia Liu<sup>a</sup>, Fang Qin<sup>b</sup>, Fen Wang<sup>a</sup>, Weiwei Chen<sup>a</sup>

<sup>a</sup> Department of Physics, Tianjin University, Tianjin 300072, China

<sup>b</sup> Department of Physics, Chengde National Teacher's College, Chengde 067000, China

## ARTICLE INFO

### Article history:

Received 14 January 2009

Received in revised form

22 April 2009

Accepted 23 April 2009

### PACS:

61.72.jn

61.72.S-

78.20.-e

### Keywords:

OH<sup>-</sup>-doped KBr polycrystal

Electrolytic coloration

Color center

## ABSTRACT

OH<sup>-</sup>-doped KBr polycrystals were colored electrolytically by using a pointed cathode and a flat anode. Characteristic O<sup>-</sup>, OH<sup>-</sup>, U, Cu<sup>+</sup> and O<sup>2-</sup>-V<sub>a</sub><sup>+</sup> absorption peaks were observed in resolved absorption spectrum of uncolored polycrystals. Herein the position of the O<sup>2-</sup>-V<sub>a</sub><sup>+</sup> absorption peak at room temperature was determined by using a Mollwo-Ivey plot. Characteristic V<sub>2</sub>, V<sub>3</sub>, Cu<sup>+</sup>, O<sup>2-</sup>-V<sub>a</sub><sup>+</sup>, I<sub>2</sub><sup>-</sup>, I<sub>2</sub> and F spectral bands were observed in Kubelka-Munk functions of colored polycrystals. Current-time curve for electrolytic coloration of an OH<sup>-</sup>-doped KBr polycrystal and its relationship with electrolytic coloration process were given. Formation and conversion of color centers were explained.

© 2009 Elsevier B.V. All rights reserved.

## 1. Introduction

In optoelectronic research, it is very basic and important to search proper materials and preparation methods, and related researches have never been discontinued [1–13]. Among various optoelectronic materials, some alkali halide hosts have good optical properties, and they have been at the center of much attention, in particular to doped ones. Indeed, the OH<sup>-</sup>-doped KBr hosts have very good optical properties and the corresponding colored ones are well-known optoelectronic materials. In past researches, much attention has been paid to single crystals but little to polycrystals. Production and spectral property of color centers in polycrystals are nearly identical with those in single crystals. However, polycrystals can be prepared more conveniently and quickly by slowly cooling the melt rather than by growing single crystals. The corresponding single crystal may not be commercially available or cannot be grown easily. Practically, the method of the polycrystal preparation is a very effective and convenient method for research and application of color centers in some hosts.

OH<sup>-</sup>-doped KBr single crystals can be colored by additive coloration or ionized radiation [14,15] but, as is well known, also electrolysis is a very effective and convenient method for producing color centers in various single crystals. In past

electrolysis researches, it was believed impossible to color directly electrolytically OH<sup>-</sup>-doped KBr hosts because the doped OH<sup>-</sup> impurities were the impassable obstacle to the formation of the secondary alkali cathode. The formation of the secondary alkali cathode was a very necessary condition to start electrolytic coloration through mode of electron injection under using a pointed cathode and a flat anode. Therefore, no electrolytic coloration for OH<sup>-</sup>-doped KBr host has been performed heretofore. However, our present results show that the previous problem to prevent the electrolytic coloration of the OH<sup>-</sup>-doped KBr host has been solved by using a homemade electrolysis apparatus. OH<sup>-</sup>-doped KBr polycrystals were effectively colored electrolytically under various coloration temperatures and voltages. Characteristic V<sub>2</sub>, V<sub>3</sub>, Cu<sup>+</sup>, O<sup>2-</sup>-V<sub>a</sub><sup>+</sup>, I<sub>2</sub><sup>-</sup>, I<sub>2</sub> and F spectral bands were observed simultaneously in the Kubelka-Munk (K-M) functions of the colored polycrystals.

## 2. Research details

KOH and KBr (contents of remnant copper and iodide impurities are 0.001 and 0.003 wt%, respectively) in wt ratio of 1:10 or 1:5 were mixed adequately. The mixture was melted in air and slowly cooled to room temperature (RT), then a block OH<sup>-</sup>-doped KBr polycrystal was obtained. Samples of size 10 × 9 × 0.5 (for absorption spectral measurement) or 10 × 9 × 5 (for electrolytic coloration) mm<sup>3</sup> were cut from the polycrystal block and polished.

\* Corresponding author. Tel.: +86 022 2789 1344; fax: +86 022 2789 0681.  
E-mail address: [jthgu@163.com](mailto:jthgu@163.com) (H. Gu).

Samples were colored electrolytically at various temperatures and DC voltages with the same electrolysis apparatus as the previously used one [16], by using a pointed tungsten cathode and a flat stainless-steel anode. Temperature range is from 400 to 600 °C, and voltage range from 300 to 1500 V. Some coarse graphite powders damped with alcohol was used between sample and anode for ensuring good electric contact. The sample was held in slowly flowed dry and pure nitrogen in process of electrolytic coloration. The samples were put on a copper bulk for quenching to RT after the electrolytic coloration. Absorption spectrum of uncolored samples was measured with a UV-240 spectrophotometer at RT. Because the transparency of the colored polycrystal was not very high, reflection spectral measurement was used. The reflection spectrum was measured with the same spectrophotometer at RT. The corresponding K–M function  $(1 - R)^2 / (2R)$  [17] (where  $R$  is the reflectance) was calculated from the data of the measured reflection spectrum because the K–M function is directly proportional to concentration. The K–M function was plotted against wavelength.

### 3. Main results

A typical absorption spectrum (solid curve) of an as-prepared  $\text{OH}^-$ -doped KBr polycrystal before electrolytic coloration is shown in Fig. 1. The high-energy side of the absorption spectrum can be resolved into five Gaussian-type characteristic absorption peaks (dashed curves). The absorption spectrum was plotted against photon energy in the resolution procedure. The absorption spectrum and resolved absorption peaks were replotted against light wavelength after the resolution. The corresponding peak position, width and color center type are given in Table 1. The 195, 214 and 228 nm absorption peaks are associated to the  $\text{O}^-$ ,  $\text{OH}^-$  and U absorption bands, respectively [18–20]. The 265 nm absorption peak is associated to the  $\text{Cu}^+$  absorption band [21]. The corresponding copper impurities derive from the copper remnant in the original KBr material. The 285 nm absorption peak may be associated to the absorption band of the  $\text{O}^{2-} - \text{V}_a^+$  dipoles. However, the corresponding spectral value of the  $\text{O}^{2-} - \text{V}_a^+$  dipoles in the KBr host at RT is absent in the literature. The peak wavelength of the 285 nm absorption peak is very consistent with the expected position on a Mollwo–Ivey plot of the positions of the absorption bands of the  $\text{O}^{2-} - \text{V}_a^+$  dipoles in the other alkali halide hosts at RT (see Fig. 2). Therefore, the 285 nm absorption

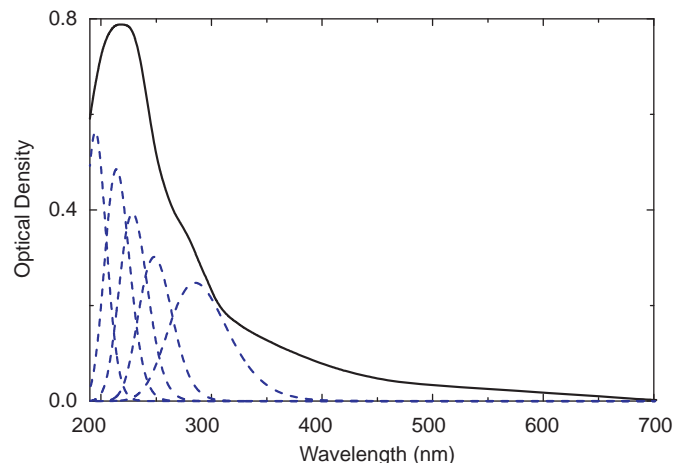


Fig. 1. The absorption spectrum (solid curve) measured from an as-prepared  $\text{OH}^-$ -doped KBr polycrystal is plotted against wavelength. Dashed curves show resolved absorption peaks.

Table 1  
Peak position, width and color center type of resolved peaks of absorption spectrum in Fig. 1.

Peak position (eV)/(nm)	Width (eV)	Color center type	Ref.
6.374/195	0.60	$\text{O}^-$	[18]
5.809/214	0.60	$\text{OH}^-$	[19]
5.452/228	0.60	U	[20]
4.691/265	0.60	$\text{Cu}^+$	[21]
4.362/285	0.80	$\text{O}^{2-} - \text{V}_a^+$	This work

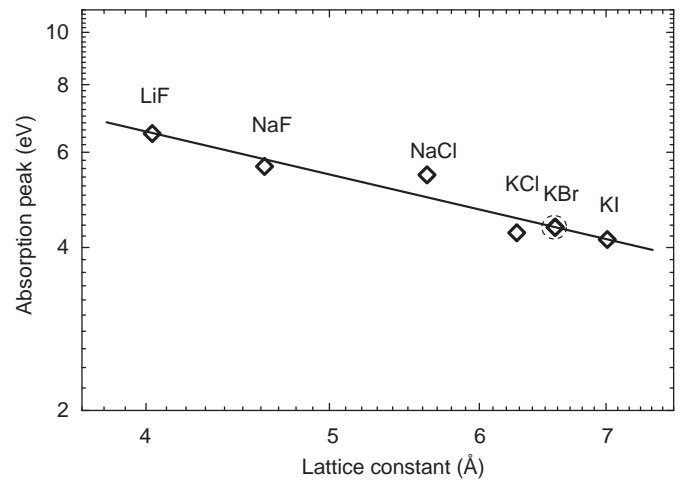


Fig. 2. Mollwo–Ivey plot for absorption bands of  $\text{O}^{2-} - \text{V}_a^+$  dipoles in various alkali halide hosts at RT.

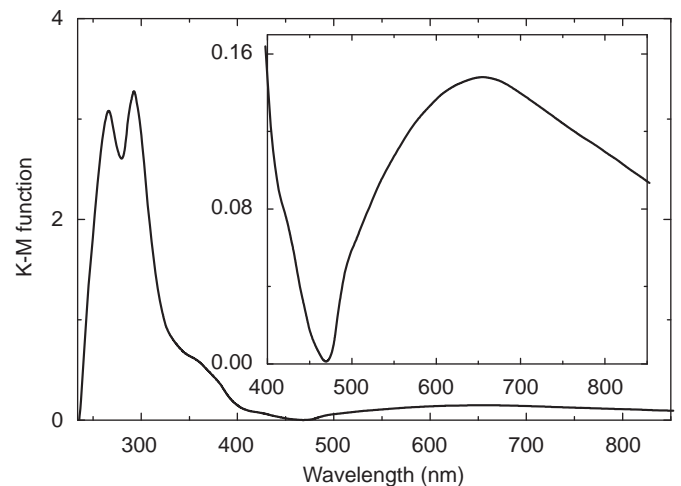
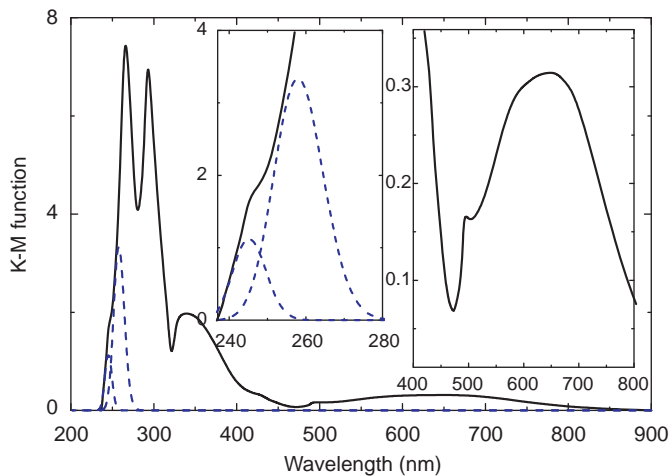


Fig. 3. The K–M function calculated from data of the reflection spectrum measured from an as-prepared  $\text{OH}^-$ -doped KBr polycrystal colored electrolytically at 433 °C and 600 V for 100 min is plotted against wavelength. Inset shows a local enlarged curve.

peak is associated most probably to the  $\text{O}^{2-} - \text{V}_a^+$  dipoles in the KBr hosts.

Fig. 3 depicts a typical K–M function calculated from data of the reflection spectrum measured from an as-prepared  $\text{OH}^-$ -doped KBr polycrystal colored electrolytically at temperature 433 °C and voltage 600 V for 100 min. The 266, 292, 360, 495 and 656 nm spectral bands are associated to the  $\text{Cu}^+$ ,  $\text{O}^{2-} - \text{V}_a^+$ ,  $\text{I}_2^-$ ,  $\text{I}_2$  and F absorption spectral bands, respectively [21–24]. The corresponding iodine impurities derive from the iodide remnant in the original KBr material.



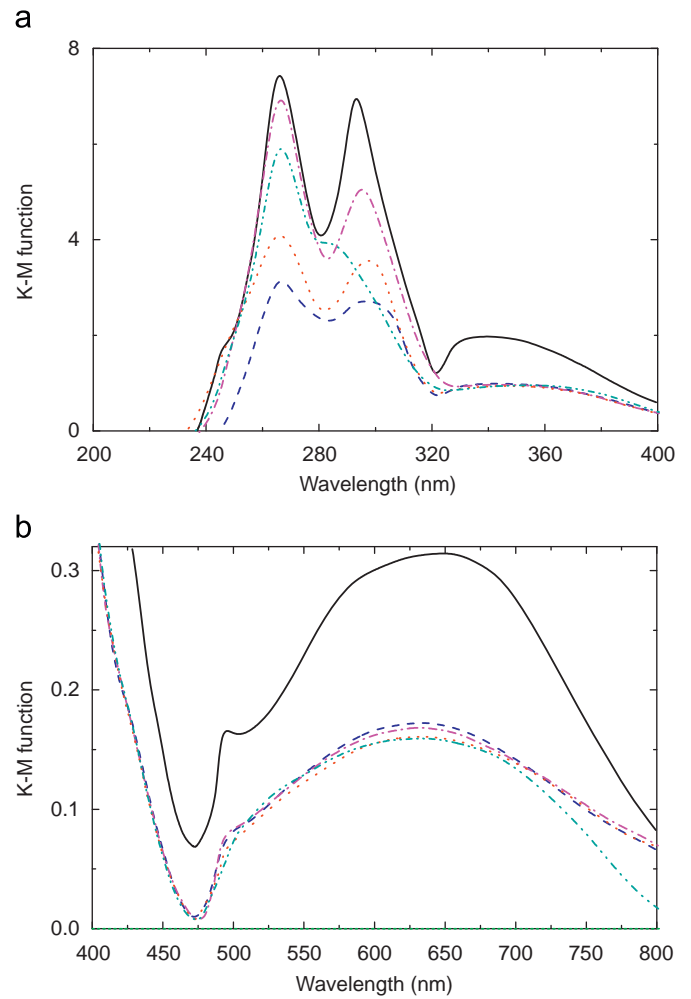
**Fig. 4.** K–M functions calculated from data of reflection spectra measured from an as-prepared  $\text{OH}^-$ -doped KBr polycrystal colored electrolytically at  $440^\circ\text{C}$  and  $900\text{V}$  for 100 min are plotted against wavelength. Solid curve shows the K–M function of the as-colored polycrystal. Dashed curves show resolved spectral peaks. Inserts show local enlarged curves.

Fig. 4 shows a typical K–M function (solid curve) calculated from data of the reflection spectrum measured from an as-prepared  $\text{OH}^-$ -doped KBr polycrystal colored electrolytically at temperature  $440^\circ\text{C}$  and voltage  $900\text{V}$  for 100 min. The 240 nm spectral band is associated to the  $V_3$  absorption bands, and the 265 nm spectral band to the  $V_2$  and  $\text{Cu}^+$  absorption bands [24]. The  $V_3$  and  $V_2$  spectral peaks are located at 245 and 258 nm in the resolved spectral curves (dashed curves) of the high-energy side of the K–M function. The corresponding widths are 0.15 and 0.22 eV, respectively. Similarly, the K–M function was plotted against photon energy in the resolution procedure. The K–M function and resolved curves were replotted against light wavelength after the resolution. The 294, 340, 495 and 650 nm spectral bands are associated to the  $\text{O}^{2-}-V_a^+$ ,  $I_2^-$ ,  $I_2$  and F absorption bands, respectively. After the colored polycrystal was stored in the dry and dark atmosphere at RT for 20 min, the K–M functions (dashed curves in Figs. 5a and b) of the colored polycrystal show that all the above spectral bands decrease. After the colored polycrystal was stored for longer time, the K–M functions of the colored polycrystal show that the F and  $I_2$  spectral bands decrease very slowly (see dash-dot, dot and dash-dot-dot curves in Fig. 5b). Therefore, the stability of the F color centers in the colored polycrystal is comparatively high.

A typical current–time curve for electrolytic coloration of an as-prepared  $\text{OH}^-$ -doped KBr polycrystal by using a pointed cathode and a flat anode at coloration temperature  $460^\circ\text{C}$  and voltage  $1500\text{V}$  is presented in Fig. 6. The current–time curve of the polycrystal is very similar to that of the single crystal [25], and displays three different zone regimes, as indicated.

#### 4. Discussion

Characteristic V ( $V_2$  and  $V_3$ ) and F spectral bands are observed in K–M functions of  $\text{OH}^-$ -doped KBr polycrystals colored electrolytically at various coloration temperatures and voltages. This observed result reveals that more V and F color centers have been produced in the colored polycrystals. In traditional opinion, an anion-doped single crystal such  $\text{OH}^-$ -doped KBr single crystal could not be colored electrolytically directly by using a pointed cathode and a flat anode. The reason was that the doped anionic impurities or their dissociated products could prevent the formation of the secondary alkali cathode. The formation of the



**Fig. 5.** K–M functions calculated from data of reflection spectra measured from the same polycrystal as in Fig. 4 are plotted against wavelength. The solid curve shows the K–M function of the as-colored polycrystal. Dashed, dash-dot, dot and dash-dot-dot curves show the K–M functions of the polycrystal after 20, 50, 80 and 420 min storage in the dry and dark atmosphere at RT, respectively. (a) The short wavelength side of the K–M functions. (b) The long wavelength side of the K–M functions.

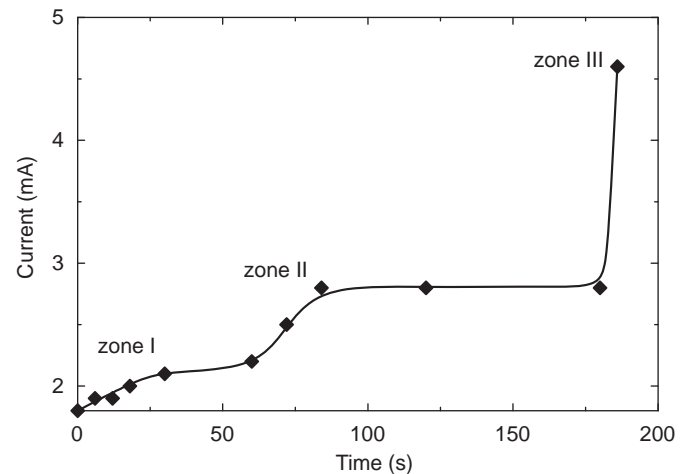


**Fig. 6.** Current–time curve for electrolytic coloration of an as-prepared  $\text{OH}^-$ -doped KBr polycrystal by using a pointed cathode and a flat anode at  $460^\circ\text{C}$  and  $1500\text{V}$ .

secondary alkali cathode was a very necessary condition to start the electrolytic coloration through the mode of the electron injection. Therefore, the realization of the present electrolytic coloration of the polycrystal is not through the mode of the electron injection. In our previous electrolysis research of OH<sup>-</sup>-doped NaCl single crystal [26], an electrolysis model was described. Namely, V color centers were produced firstly from the crystal region nearby graphite anode matrix through electron exchange. The electron exchange occurred between halogen ions and graphite anode matrix. The production of the V color centers did not need the formation of the secondary alkali cathode. F color centers were produced secondly through the photoconversion of the V color centers under light illumination. Therein, the coarse graphite grains structured the graphite anode matrix. The graphite anode matrix played a key role for starting and standing the electrolytic coloration. Therefore, we think that such an electrolysis mode is very suitable for the present electrolytic coloration of the OH<sup>-</sup>-doped KBr polycrystal although there are some differences between the polycrystal and single crystal in respect of the structure and property. Namely, V color centers are produced firstly in the coloring OH<sup>-</sup>-doped KBr polycrystal. F color centers are produced secondly through the photoconversion of the V color centers. The V color center migrates through the electron exchange of the interstitial halogen atom in the V color center, which results in the coloration of the other region of the polycrystal.

During electrolytic coloration, current–time data of OH<sup>-</sup>-doped KBr polycrystal were recorded, and current–time curve was plotted according to current–time data. From the current–time curve, one can see that the property of the current–time curve of the polycrystal is very similar to that of the single crystal [26]. Therefore, we think that the basic relationship mode between the current–time curve and electrolytic coloration process of the single crystal is very suitable for the present electrolytic coloration process of the polycrystal. That is, V color centers can be produced in the whole process of the electrolytic coloration of the OH<sup>-</sup>-doped KBr polycrystal through the electron exchange. The electron exchanges can induce a part of the current in the whole process of the electrolytic coloration. Similarly, the ionic motion under the action of the applied voltage at high temperature can induce a part of the current in the whole process of the electrolytic coloration, too. The current component induced by the ionic motion is dominant in the first-zone current. The current component induced by the electron exchange is dominant in the current of the other zones. Some V color centers were produced in the time interval of the first current zone. More V color centers were produced by the “snowslide” effect [26] in the time intervals of the other current zones. In addition, herein current undulations also result from electrode effect [26].

In polycrystal preparation, KOH is directly melted in KBr material. Some OH<sup>-</sup> impurities are dissociated, and possible reactions are as OH<sup>-</sup> → O<sup>-</sup> + H<sup>0</sup> and OH<sup>-</sup> → O<sup>2-</sup> + H<sup>+</sup>. An O<sup>-</sup> ion may trap an electron to form an O<sup>2-</sup> ion: O<sup>-</sup> + e<sup>-</sup> → O<sup>2-</sup>. An O<sup>2-</sup> ion may react with an anionic vacancy (V<sub>a</sub><sup>+</sup>) to form an O<sup>2-</sup>–V<sub>a</sub><sup>+</sup> dipole: O<sup>2-</sup> + V<sub>a</sub><sup>+</sup> → O<sup>2-</sup>–V<sub>a</sub><sup>+</sup>. The interstitial H<sup>0</sup> atom is unstable at RT or above, and it may trap an electron and enter a lattice site to form a substitutional H<sup>-</sup> ion, i.e., a U color center. Hence, the absorption peaks of the O<sup>-</sup> ions, O<sup>2-</sup>–V<sub>a</sub><sup>+</sup> dipoles and U color centers appear in the resolved absorption spectrum of the uncolored polycrystal (see Fig. 1). After electrolytic coloration, some O<sup>2-</sup>–V<sub>a</sub><sup>+</sup> dipoles still exist in colored polycrystals because the spectral bands of the O<sup>2-</sup>–V<sub>a</sub><sup>+</sup> dipoles were observed in the K–M functions of the colored polycrystals (see Figs. 3 and 4).

Obviously, the useful O<sup>2-</sup>–V<sub>a</sub><sup>+</sup> dipoles and V, F color centers are produced simultaneously in an electrolytically colored OH<sup>-</sup>-doped KBr polycrystal only through a simple electrolysis process. These dipoles and color centers may be very significant for further research and application of colored polycrystals.

## 5. Conclusion

OH<sup>-</sup>-doped KBr polycrystals were colored electrolytically by using a pointed cathode and a flat anode. V<sub>2</sub> and V<sub>3</sub> color centers were directly produced during the whole process of the electrolytic coloration. Some V<sub>2</sub> and V<sub>3</sub> color centers were produced in the time interval of the first current zone. More V<sub>2</sub> and V<sub>3</sub> color centers were produced in the time intervals of the other current zones. The V<sub>2</sub> and V<sub>3</sub> color centers migrated through the electron exchange, and F color centers were formed by photoconversion of the V<sub>2</sub> and V<sub>3</sub> color centers under light illumination. The current of the electrolytic coloration consisted of the two current components induced by the electron exchange and ionic motion. The current component induced by the ionic motion was dominant in the first-zone current, while the current component induced by the electron exchange was dominant in the current of the other zones.

## Acknowledgment

This work was partly supported by the National Natural Science Foundation of China under Grant nos. 69178028 and 70120001.

## References

- [1] R.A. Nunes, A.P. da Silva Sotero, L.C. Scavarda do Carmo, M. Cremona, R.M. Montereali, M. Rossi, F. Somma, J. Lumin. 60–61 (1994) 552.
- [2] M. Cremona, A.P. da Silva Sotero, R.A. Nunes, M.H.D. Mauricio, L.C. Scavarda do Carmo, R.M. Montereali, S. Martelli, F. Somma, Rad. Eff. Def. Sol. 136 (1995) 1073.
- [3] C.B. Jiang, B. Wu, Z.Q. Zhang, L. Lu, S.X. Li, Appl. Phys. Lett. 88 (2000) 093103.
- [4] M. Cremona, C.A. Achete, P.I. Guimaraes, Thin Solid Films 398 (2001) 349.
- [5] P.A. Burns, J.M. Dawes, P. Dekker, J.A. Piper, J. Li, J.Y. Wang, Opt. Commun. 207 (2002) 315.
- [6] T. Marolo, G. Baldacchini, V.S. Kalinov, R.M. Montereali, Phys. Status Solidi C 2 (2005) 367.
- [7] F. Chen, X.L. Wang, K.M. Wang, Opt. Mater. 29 (2007) 1523.
- [8] F. Barkusky, C. Peth, A. Bayer, K. Mann, J. Appl. Phys. 101 (2007) 124908.
- [9] G.H. Cheng, Y.S. Wang, J.F. He, G.F. Chen, W. Zhao, Opt. Express 15 (2007) 8938.
- [10] H. Kim, A.H. King, J. Mater. Res. 23 (2008) 452.
- [11] T. Kurobori, Y. Obayashi, M. Kurashima, Y. Hirose, T. Sakai, S. Aoshima, T. Kojima, S. Okuda, Nucl. Instrum. Meth. B 266 (2008) 2762.
- [12] T. Kurobori, Y. Obayashi, K. Suzuki, Y. Hirose, T. Sakai, S. Aoshima, Jpn. J. Appl. Phys. 47 (2008) 685.
- [13] Y. Obayashi, T. Kurobori, Y. Hirose, T. Sakai, S. Aoshima, Rev. Laser Eng. 36 (2008) 1226.
- [14] J. Rolfe, Phys. Rev. Lett. 1 (1958) 56.
- [15] G. Baldacchini, S. Botti, U.M. Grassano, L. Gomes, F. Lüty, Europhys. Lett. 9 (1989) 735.
- [16] C.Y. Song, H.E. Gu, L. Han, Y.R. Wu, Phys. Status Solidi A 202 (2005) 140.
- [17] G. Kortüm, Reflectance Spectroscopy, Springer, Berlin, 1969.
- [18] L. Gomes, S.P. Morato, Phys. Rev. B 55 (1997) 8743.
- [19] H.W. Etzel, D.A. Patterson, Phys. Rev. 112 (1958) 1112.
- [20] F. Kerkhoff, W. Martienssen, W. Sander, Z. Phys. 173 (1963) 184.
- [21] K. Fussaenger, Phys. Status Solidi 34 (1969) 157.
- [22] C.J. Delbecq, W. Hayes, P.H. Yuster, Phys. Rev. 121 (1961) 1043.
- [23] H.N. Hersh, Phys. Rev. 105 (1957) 1410.
- [24] R. Casler, P. Pringsheim, P. Yuster, J. Chem. Phys. 18 (1950) 1564.
- [25] C.Y. Song, H.E. Gu, Y.R. Wu, L. Han, J. Lumin. 113 (2005) 169.
- [26] H.E. Gu, C.Y. Song, L. Han, J. Lumin. 117 (2006) 123.